MRS Advances © 2019 Materials Research Society
DOI: 10.1557/adv.2019.47

Size-Controlled Synthesis of CuNi Nano-Octahedra and Their Catalytic Performance towards 4-Nitrophenol Reduction Reaction

Can Li[1], Yiliang Luan[1], Bo Zhao[2], Amar Kumbhar[3], Jiye Fang[1*]

[1]*Department of Chemistry, State University of New York at Binghamton, New York, USA.*

[2]*College of Arts & Sciences Microscopy, Texas Tech University, Texas, USA.*

[3]*Chapel Hill Analytical and Nanofabrication Laboratory, University of North Carolina at Chapel Hill, North Carolina, USA.*

Abstract

In this work, we demonstrate a size-controlled synthesis of CuNi octahedral nanocrystals (NCs) using a hot colloidal solution approach. Two different sizes of CuNi nano-octahedra are chosen and investigated. It is determined that the reagent concentration remarkably plays a key role in the formation of the size-defined CuNi octahedral NCs. In terms of the reduction of 4-nitrophenol (4-NP), it uncovers that the obtained CuNi octahedral NCs (in both sizes) exhibit higher catalytic activity than those of CuNi spherical NCs reported previously. It further indicates that the catalytic performance is strongly size-dependent due to their devise specific surface areas of the exposed crystallographic planes.

INTRODUCTION

Bimetallic materials have attracted more attention than monometallic elements due to their unique performance toward catalysis. It has been reported that the catalytic performance of bimetallic nanocrystals (NCs) is highly dependent on their sizes, composition, and morphology[1-6]. However, most of the reported bimetallic NCs are noble metal-based nanocatalysts. Compared with these NCs, non-precious metal catalyst (NPMC) NCs as a class of devise catalysts have shown an unprecedented level of interest due to their low cost, abundant content in the Earth's crust, and comparable or outstanding catalytic performance in some reaction such as oxidation, hydrogenation, and electrocatalysis. Although it is well known that some specific crystal facets on the NCs can promote the catalytic activity, there are limited studies on the synthesis of facet- and size-controlled NPMC NCs[7-12]. Since the standard reduction potentials of the NPMCs are much lower than those of the noble metals, the relatively high sensitivity and instability of the NPMC NCs, especially when exposed to air or aqueous solution, make it hard to control both the crystal size and shape in their preparation process. Thus, synthesis of facet- (or shape-) and size-defined NPMC NCs still remain a challenge.

In this study, we focus on two different sizes of CuNi nano-octahedral NCs prepared in a hot colloidal solution using borane morpholine (BM) as a reducing reagent as well as the capping ligand to promote rapid nucleation and to control the exposed crystallographic facets. It was identified that the concentrations of BM and Cu-/Ni-precursors remarkably affected the size of the resultant CuNi nano-octahedral NCs, which was not studied previously. The synthesized CuNi nano-octahedra in both sizes were further evaluated as catalysts in 4-nitrophenol (4-NP) reduction, a model reaction, to investigate their shape- and size-dependent catalytic performance and to compare with that of CuNi nano-spheres/polyhedrons. Results show that 10 nm CuNi octahedral catalysts exhibit higher activity compared with that of the analog in 20 nm, indicating that the former should possess more active sites due to its higher specific surface area.

EXPERIMENT

Synthesis of CuNi bimetallic nano-octahedra

10 nm CuNi nano-octahedra were prepared using a modified synthetic method[12]. First, a BM solution, as a reducing agent was freshly prepared using the following recipe: 0.1816 g of BM pellets were introduced into a degassed mixture (*vide infra*) containing 2.50 mL of diphenyl ether (DPE), 1.70 mL of oleylamine (OLA) and 0.34 mL of oleic acid (OA). In a typical synthesis of 10 nm CuNi nano-octahedra, 0.05 mmol of cupric(II) acetylacetonate and 0.05 mmol of nickel (II) acetylacetonate were dissolved in a mixture consisting of 2.50 mL of DPE, 1.70 mL of OLA and 0.34 mL of OA. The crystal blue solution was degassed under vacuum at 90 ℃ for 1 hour before the temperature was raised to 240 ℃ within 12 min. The freshly prepared BM solution (0.50 mL) was then injected into the Cu-Ni precursor solution at 240 ℃ promptly, accompanying a color change of the mixture to dark brown quickly. After the reaction system was further evolved for an additional 20 min at 240 ℃, it was cooled to room temperature and the products were isolated by adding a given amount of anhydrous ethanol followed by centrifugation. The 10 nm CuNi nano-octahedra were purified by a re-dispersion of the NCs in hexane and addition of the ethanol followed centrifugation for three cycles, and the NCs were finally dispersed in hexane as stock suspensions.

The synthetic procedure of 20 nm CuNi nano-octahedra is similar, except for a new recipe for DPE, OLA and OA, which are 5.00 mL, 3.40 mL, and 0.68 mL, respectively. The 12 nm CuNi nano-spheres were synthesized by introducing tri-octyl phosphine(TOP) as capping ligand, similar to the synthesis method reported previously except increasing TOP volume to 1.50 mL [11]. X-ray diffraction patterns were collected using a PANalytical X'pert X-ray powder diffractometer equipped with a Cu Kα_1 radiation source. Inductively coupled plasma-optical emission spectrometry (ICP-OES) was carried out on an optima 7000 DV ICP-OES spectrometer (PerkinElmer). The compositions for 10 nm CuNi octahedra, 20 nm CuNi octahedra, and CuNi nano-spheres were analyzed by ICP and their atomic ratio of Cu and Ni were calculated as 53:47, 52:48 and 50:50, respectively, suggesting the compositions of the three catalysts were almost the same.

Catalytic activity evaluation of 4-NP reduction reaction

The as-prepared CuNi bimetallic NCs were loaded on carbon black (Vulcan xc72) with a total metal fraction of 50 wt% using a standard procedure[5]. The catalysts (CuNi NCs/C) were re-dispersed in ethanol completely after a sufficient ultra-sonication manipulation and the concentration of the metal catalysts was determined as 1.0 mg/mL. The reaction setup was similar to that reported in our previous work[4]. In a typical experiment, 30.6 mg of sodium borohydride ($NaBH_4$) was dissolved into 8.0 mL of ultrapure water cooled in an ice bath. 40.0 μL of the as-prepared catalyst suspensions in ethanol was added under vigorous stirring. Subsequently, 300 μL of 4-NP (10 mmol/L) solution was rapidly injected. The bright yellowish color of the solution started to fade, indicating an occurrence of the reduction reaction. The progress of 4-NP reduction reaction was monitored by Ultraviolet/visible (UV/Vis) absorption spectra of the mixture after a dilution. According to Lamber-Beer's Law, A_t/A_0 was converted into the retained concentration (C_t) of 4-NP, where A_t and A_0 represent the absorbance at 400 nm at a specific time and the initial time respectively. The apparent rate constants (k) for the pseudo-first order reaction under different catalysts can consequently be obtained from the slope of $lnC_t - t$ plots and the k/m ($s^{-1}\cdot g^{-1}$) can be further calculated.

RESULTS AND DISCUSSION

Size-controlled synthesis of CuNi NCs

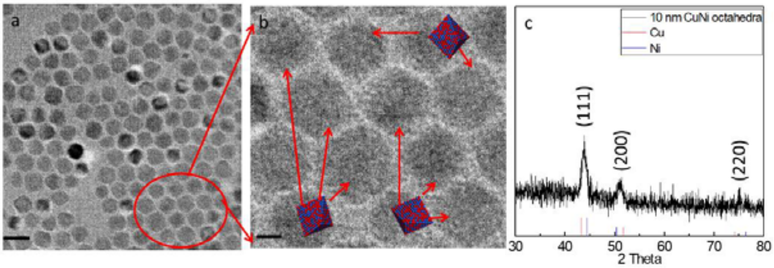

Figure 1. TEM images (a, b) and XRD pattern (c) of 10 nm CuNi nano-octahedra. The red atoms in CuNi octahedral models inserted in (b) stand for Cu and the blue atoms for Ni. The scale bar in each image represents 20 nm. The red and blue lines on the bottom of (c) show standard XRD patterns of Cu and Ni (ICDD PDF cards 00-001-1241, 00-001-1258), respectively.

A facile synthesis method was utilized to prepare the CuNi nano-octahedra in both sizes, after a slight modification according to the previous study[12]. The average particle sizes of both samples were determined as 10 nm and 20 nm, respectively, based on the TEM observation (Figures 1 & 2). As shown in Figures 1 & 2, each specific XRD peak of all the CuNi octahedra and spheres falls into a position spanned between the corresponding peaks of pure Cu and Ni, indicating the character of CuNi composite. It is well known that the synthesis consists of a nucleation stage (seed formation) and crystal growth stage (NC formation). In this system, the nucleation kinetics plays a key role in controlling the size of CuNi nano-octahedra. By introducing BM as a reducing agent into the colloidal system at a high temperature, large amounts of Cu-Ni seeds rapidly boomed and reach a high concentration in this nucleation stage, promoted by this relatively fast reduction of Cu and Ni precursors. The ad-atoms of the further reduced Cu and Ni in a limited amount could subsequently “deposit” on their preferred sites synergistically acted by OLA and OA, remaining the {111} facets as stable planes and generating 10 nm CuNi octahedral NCs (Figure 1a). When the volumes of DPE, OLA and OA were proportionally doubled, it is believed that the conditions of octahedral NC formation controlled by the capping ligands shouldn’t be altered much. However, the low concentration of BM (due to the double of the solution volume) deaccelerates the Cu-Ni seed formation during the nucleation stage. Once the “first batch” of Cu-Ni seeds are generated from the solution, the concentration of “free” Cu and Ni atoms will reduce from their saturated (or supersaturated) environment and there is no reason to produce a second batch of Cu-Ni seeds in this “closed system”. The remainder of Cu and Ni precursors, which are believed more than that in the former case, will be gradually reduced by the equal amount of BM used in the former case and these Cu/Ni-free atoms will have to deposited onto the Cu-Ni seeds that present in a low concentration compared with the former case, yielding large-sized products (20 nm, Figure 2a & 2b).

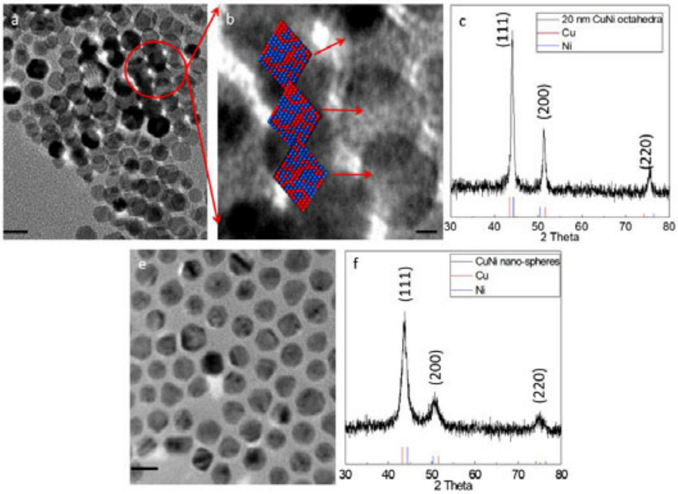

Figure 2. TEM images (a, b) and XRD pattern (c) of 20 nm CuNi nano-octahedra, as well as TEM image (e) and XRD pattern (f) of 12 nm CuNi nano-spheres. The red atoms in CuNi octahedral models inserted in (b) stand for Cu and the blue atoms for Ni. The scan bar represents 20 nm in (a) or (e) and 5 nm in (b), respectively. The red and blue lines on the bottom of (c) show standard XRD patterns of Cu and Ni (ICDD PDF cards 00-001-1241, 00-001-1258), respectively.

Catalytic performance

The conversion of toxic 4-NP to less toxic 4-aminophenol as a useful intermediate is a meaningful way in many drug manufacturing designs. To examine the size-effect, both sizes of the carbon-loaded CuNi samples (10 nm and 20 nm) were tested by the 4-NP reduction reaction in the presence of $NaBH_4$ to compare their catalytic activity. UV/Vis spectroscopy was used to monitor the reduction progress. As shown in Figure 3, the absorption peaks at a wavelength of 400 nm in the UV/Vis spectra are ascribed to the 4-NP[4]. The intensity of this peak was maintained unchanged in a blank experiment even remaining for 1 hour, indicating that no reduction reaction occurred in the absence of the metal catalysts. After 20 μL of the 10 nm (or 20 nm) CuNi NC/C suspensions were injected, the intensity of the absorption peak of 4-NP in the time-resolved UV/Vis spectra gradually decreased as the reduction reaction proceeded in a short time, suggesting a high effectiveness of CuNi NCs as an excellent type of NPMC nano-catalysts. The negligible absorbance at 400 nm, in the end, indicated that 4-NP was almost converted to 4-aminophenol.

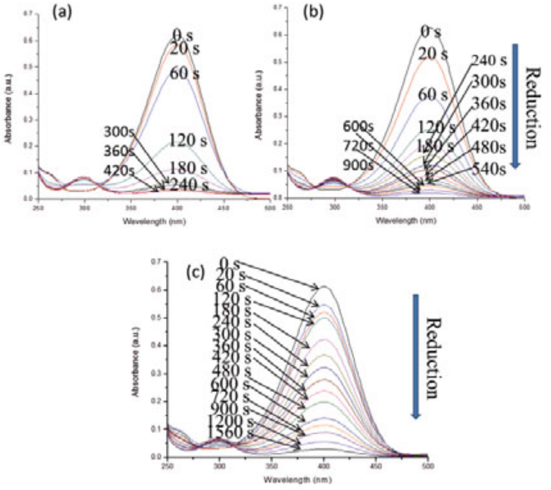

Figure 3. Time-resolved UV/Vis absorption spectra of 4-NP reduction by $NaBH_4$ in the presence of (a) 10 nm CuNi octahedral NCs/C, (b) 20 nm CuNi octahedral NCs/C, and (c) 10 nm CuNi nano-spheres NCs/C.

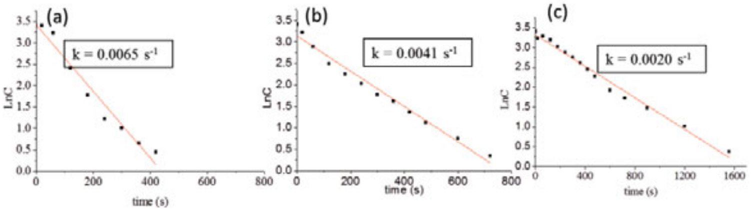

Figure 4. A linear relationship between the logarithmic concentration of 4-NP and the time with a rate constant k obtained from the slope in the presence of (a) 10 nm CuNi octahedral NCs/C, (b) 20 nm CuNi octahedral NCs/C, and (c) 10 nm CuNi nano-spheres NCs/C.

Since the amount of $NaBH_4$ used in the discussed experiments greatly exceeded the stoichiometric equivalent that is needed for the 4-NP reduction, the concentration of $NaBH_4$ can be assumed as a constant during this reaction. Thus, pseudo-first-order kinetics with respect to 4-NP reduction is applied for determining the rate constant. The apparent rate constant k is obtained by plotting of $ln(C_t)$ versus t after converting A_t to C_t

using the Lamber-Beer's Law. As a result (shown in Figure 4), the 10 nm CuNi NCs exhibited a *k* value of 0.0065 s^{-1} and a *k/m* value of 163 $s^{-1}\cdot g^{-1}$, whereas the 20 nm CuNi NCs gave a *k* value of 0.0041 s^{-1} and a *k/m* value of 103 $s^{-1}\cdot g^{-1}$, indicating that the former possesses a higher catalytic activity in terms of the 4-NP reduction reaction. This can be explained as that 10 nm CuNi NCs contained larger specific surface area than that of 20 nm CuNi NCs, providing more catalytic sites for accommodating the 4-NP reduction reaction. In terms of the shape-effect toward 4-NP reduction, both of the catalysts showed higher activity than the CuNi nano-spheres/C with a *k* value of 0.0020 s^{-1}, revealing that the catalytic performance of CuNi NCs is also shape-dependent. It is believed that the reactants such as 4-NP and H_2 are most likely easier to adsorb on the {111} facets that are dominant surfaces in the octahedral nano-catalysts, whereas the surfaces of spherical nano-catalysts are composed of polycrystalline facets as an opposite case. Therefore, the {111}-terminated CuNi catalysts lead to superior 4-NP reduction kinetics.

CONCLUSIONS

In summary, CuNi octahedral NCs (two sizes) were synthesized using a high-temperature colloidal method. We utilized the nucleation kinetics to control the size of the CuNi NCs. When the amounts of the reagents are fixed, a high concentration of reducing agent could generate a high concentration of CuNi seeds/nuclei with less precursor resource for further particle growth; *or vice versa*. The catalytic study reveals that CuNi octahedral NCs/C catalysts in both sizes exhibited high catalytic activities toward the 4-NP reduction reaction. Furthermore, 10 nm CuNi octahedral NCs/C showed higher activity than the 20 nm counterpart possibly due to its high density of catalytic sites.

ACKNOWLEDGMENTS

This work was supported by ACS PRF (58196-ND10) and NSF (DMR-1808383), and S3IP at Binghamton University. We thank I. –T Bae for his TEM training and assistance. We thank Professor David M. Jenkins and David Collins for their support in the X-ray diffraction analysis.

REFERENCES

1. J. Zhang and J. Fang. *J. Am. Chem. Soc.* **131**, 18543-18547 (2009).
2. J. Zhang, H. Yang, J. Fang and S. Zou. *Nano Lett.* **10**, 638-644 (2010).
3. J. Zhang, H. Yang, B. Martens, Z. Luo, D. Xu, Y. Wang, S. Zou and J. Fang. *Chem. Sci.* **3**, 3302-3306 (2012).
4. C. Wang, C. Lin, B. Zhao, L. Zhang, A. Kumbhar, G. Fan, K. Sun, J. Zhang, S. Chen and J. Fang. *ChemNanoMat* **1**, 331-337 (2015).
5. C. Wang, L. Zhang, H. Yang, J. Pan, J. Liu, C. Dotse, Y. Luan, R. Gao, C. Lin, J. Zhang, J.P. Kilcrease, X. Wen, S. Zou and J. Fang. *Nano Lett.* **17**, 2204-2210 (2017).
6. Y. Luan, L. Zhang, C. Wang, J. Liu and J. Fang. *MRS Advances* **3**, 943-948 (2018).
7. S. Zhang and H.C. Zeng. *Chemistry of Materials* **22**, 1282-1284 (2010).

8. T. Yamauchi, Y. Tsukahara, T. Sakata, H. Mori, T. Yanagida, T. Kawai and Y. Wada. *Nanoscale* **2**, 515-523 (2010).

9. H. Guo, Y. Chen, H. Ping, L. Wang and D.-L. Peng. *J. Mater. Chem.* **22**, 8336-8344 (2012).

10. H. Guo, Y. Chen, H. Ping, J. Jin and D.-L. Peng. *Nanoscale* **5**, 2394-2402 (2013).

11. J. Liu, Y. Zheng and S. Hou. *RSC Adv.* **7**, 37823-37829 (2017).

12. M. Wang, L. Wang, H. Li, W. Du, M.U. Khan, S. Zhao, C. Ma, Z. Li and J. Zeng. *J. Am. Chem. Soc.* **137**, 14027-14030 (2015).